Journal of Physiology (1988), **398**, *pp.* 291–311
With 8 text-figures
Printed in Great Britain

VOLTAGE-GATED SODIUM AND CALCIUM CURRENTS IN RAT OSTEOBLASTS

BY DOMINIQUE CHESNOY-MARCHAIS* AND JANINE FRITSCH†

*From the * Laboratoire de Neurobiologie, Ecole Normale Supérieure, 46 rue d'Ulm, 75005 Paris and the †CNRS UA 583, Hôpital des Enfants-Malades, 149 rue de Sèvres 75015 Paris, France*

(Received 6 July 1987)

SUMMARY

1. The whole-cell voltage-clamp mode of the patch-clamp technique was used to investigate the presence of voltage-gated inward currents in osteoblasts from newborn rat calvaria.

2. In K^+-free solutions, three kinds of inward currents could be activated by depolarization: a voltage-gated Na^+ current and two different types of Ca^{2+} currents.

3. The Na^+ current was activated by depolarization above -40 mV in all the cells. It was reduced by half by 10 nM-TTX (tetrodotoxin).

4. In an isotonic Ba^{2+} external solution containing TTX, and with a Cs–EGTA internal solution buffered at pCa 8, depolarizing jumps induced both a transient Ba^{2+} current and a sustained Ba^{2+} current. The relative proportions of these two currents varied greatly among cells.

5. The transient and sustained Ba^{2+} currents differ with respect to their time course and their voltage dependence.

6. The depolarization-activated inward currents were also observed under more physiological conditions, in the presence of only 2 mM-external Ca^{2+} and with a K^+ internal solution buffered at pCa 7.

7. A few records obtained in current clamp showed that it is possible to induce action potentials in osteoblasts.

INTRODUCTION

Osteoblasts are the cells responsible for bone matrix formation and recent studies have shown that they are also involved in the hormonal control of bone resorption (Chambers, 1980; Rodan & Martin, 1981). Since the initial suggestions that some bone-resorbing hormones, like parathormone (PTH), might stimulate the uptake of Ca^{2+} ions into osteoblasts (Dziak & Stern, 1975; Nijweide, 1975; Marcus & Orner, 1980), several studies have suggested that the intracellular Ca^{2+} concentration might vary during hormonal responses (see Wong, 1986 for a review). Direct measurements of the intracellular Ca^{2+} concentration have been made by using the fluorescent Ca^{2+} indicator quin-2 in different cultures of 'osteoblasts' (osteoblast-like cell lines or primary cultures). Some of these studies have shown that the intracellular Ca^{2+}

concentration of osteoblasts does vary during stimulation with bone-resorbing hormones (Löwik, van Leeuwen, van der Meer, van Zeeland, Scheven & Hermann-Erlee, 1985; Lieberherr, 1987 but see Boland, Fried & Tashjian, 1986). Furthermore, in one osteoblast-like cell line (ROS25/1), but not in some others, it was shown that increasing the extracellular K^+ concentration increases the intracellular Ca^{2+} concentration, suggesting that osteoblasts might have voltage-dependent Ca^{2+} channels (Boland *et al.* 1986).

In the present study, by using the patch-clamp technique, we demonstrate the existence of two different kinds of voltage-gated Ca^{2+} currents and a TTX-sensitive voltage-gated Na^+ current in osteoblasts from newborn rat calvaria.

METHODS

The experiments were performed at room temperature on primary cultures of newborn rat osteoblasts in the whole-cell configuration of the patch-clamp technique (Hamill, Marty, Neher, Sakmann & Sigworth, 1981).

Cell preparation. Osteoblastic cells were isolated from newborn rat calvaria. While holding the animal gently on a polystyrene sheet the head was removed instantaneously with one stroke of a razor blade. As is the case in most laboratories studying bone cells, the use of anaesthetics was avoided, since they are known in particular to modify the calcemia and the alkaline phosphatase activity. The central parts of parietal bones were excised and the periosteal tissues carefully stripped away. Bones were incubated at 37 °C during two sequential 10 min periods in a Ca^{2+}–Mg^{2+}-free Earle solution containing 0·5 mg trypsin/ml (Worthington) and 4 mM-EDTA. Isolated cells were harvested, washed and seeded at about 10000 cells/dish (35 mm Falcon) in BGJ medium (Flow Laboratories) supplemented with 10% fetal calf serum (Flow Laboratories), fungizone (2·5 μg/ml), penicillin (100 i.u./ml) and streptomycin (50 μg/ml). Experiments were performed on isolated cells from day 3 to day 5 in culture.

Using the Sigma kit no. 85-1, approximately 90% of the attached cells were shown to have intense alkaline phosphatase reactivity, a well-known indicator of the osteoblastic phenotype (Rodan & Rodan, 1984).

Solutions. The culture dish was continuously perfused with the Na^+–5 K^+–1 Ca^{2+}–1 Mg^{2+} solution described in Table 1. In each experiment, the cell from which the current was recorded was locally perfused with a given external solution, by using a pipette of about 300 μm diameter placed at about 50 μm from the cell. This pipette was connected to the output of a two-way plastic tap. The compositions of the external and internal solutions are given in Table 1.

In many experiments designed for the study of the voltage-gated Ca^{2+} conductances, we used the isotonic Ba^{2+} external solution, usually supplemented with 200 nM-TTX, and the Cs–EGTA internal solution buffered at pCa 8 (Table 1). Both these solutions were K^+ free and only contained about 3 mM-Na^+, thus making very unlikely a contamination of the records by K^+ or Na^+ currents.

Even though it was possible to detect convincing transient and sustained Ca^{2+} currents in the presence of 2 mM-Ca^{2+} ions (Figs 1 and 7), the use of a high concentration of external Ba^{2+} ions greatly enhanced both currents flowing through Ca^{2+} channels, in particular the sustained current (see Fig. 7), thus allowing us to minimize possible difficulties related to the subtraction of the leak current (see below). The use of Ba^{2+} rather than Ca^{2+} ions also prevented the possible Ca^{2+}-dependent inactivation that would occur, in spite of the presence of a very high concentration of internal EGTA, if local intracellular Ca^{2+} concentration changes transiently occurred following Ca^{2+} entry. Thus, the isotonic Ba^{2+} solution facilitated the separation of the two Ca^{2+} currents and the comparison of their voltage sensitivity.

In a few experiments the CsCl internal solution, also buffered at pCa 8, was used instead of the Cs–EGTA solution and very similar results were obtained. The Cs–HEDTA or K–HEDTA solutions buffered at pCa 7 were also used in some experiments. ATP and Mg^{2+} were introduced in all internal solutions since their presence has been reported to slow (Forscher & Oxford, 1985; Byerly & Yazejian, 1986) the 'run-down' of Ca^{2+} currents which often occurs after internal dialysis.

TABLE 1. Composition of solutions (mM)

	NaCl	KCl	$MgCl_2$	$CaCl_2$ (or $BaCl_2$)	CsCl	EGTA	HEDTA
Na^+–5 K^+–1 Ca^{2+}–1 Mg^{2+}	140	5	1	1	—	—	—
Na^+–5 K^+–2 Ca^{2+}–1 Mg^{2+}	140	5	1	2	—	—	—
Na^+–2 Ca^{2+}–1 Mg^{2+}	140	0	1	2	—	—	—
Ca^{2+}	0	0	0	105	—	—	—
Ba^{2+}	0	0	0	108 ($BaCl_2$)	—	—	—
Cs–EGTA, pCa8	—	0	1	6	0 (145)	64	0
CsCl, pCa8	—	0	1	1	117 (140)	10	0
Cs–HEDTA, pCa7	—	0	1	1·5	57 (140)	0	40
K–HEDTA, pCa7	—	56 (130)	1	1·5	0	0	40

The external solutions were all buffered at pH 7·6 with 10 mM-HEPES (*N*-2-hydroxyethyl-piperazine-*N'*-2-ethane sulphonic acid-NaOH). In a few experiments, the NaCl (140 mM) of the Na^+–2 Ca^{2+}–1 Mg^{2+} solution was replaced by Tris (tris-(hydroxymethyl)-amino-methane-HCl) (154 mM) or *N*-methyl-glucamine-HCl (140 mM). The Na^+–0·5 Ca^{2+}–2·5 Mg^{2+}, Na^+–0 Ca^{2+}–1 Mg^{2+} and Na^+–0 Ca^{2+}–3 Mg^{2+} solutions contained 140 mM-NaCl and the concentrations of $CaCl_2$ and $MgCl_2$that are indicated (mM) by the names of the solutions (no EGTA (ethyleneglycol-bis-(β-amino-ethyl-ether)-*N*,*N'*-tetraacetic acid) added). The internal solutions all contained 2 mM-ATP (adenosine-5'-triphosphate disodium salt); they were all buffered at pH 7·3 with 10 mM-HEPES–NaOH. EGTA or HEDTA (*N*-hydroxyethyl-ethylene-diamine-triacetic acid) was added from solutions which were previously buffered at this pH with either CsOH (Cs–EGTA and Cs–HEDTA solutions) or KOH (K–HEDTA solution). The final concentration of Cs^+ or K^+ ions in each internal solution is indicated in parentheses. In most experiments, the internal solutions described in this Table were diluted by 10% with distilled water.

Bay K8644 (kind gift of Dr Franckowiak, Bayer AG, F.R.G.) was first diluted to 10 mM in DMSO (dimethyl sulphoxide) and (+)-PN-200-110 (kind gift of Dr Hof, Sandoz, Switzerland) was diluted to 1 mM in 95% ethanol. These stock solutions were then diluted in the Ba^{2+} solution and the corresponding concentration of DMSO or ethanol was added to the Ba^{2+} solution for controls.

Recording and analysis. Patch-clamp micropipettes were made from soft glass; the shank of each pipette was covered with Sylgard and the tip was slightly fire polished. The typical pipette resistance was about 4 MΩ when filled with the usual Cs–EGTA internal solution. The bath was grounded via an agar bridge. The junction potential between the bath and the tip of the pipette was measured and was taken into account as explained in Fenwick, Marty & Neher (1982). The current output of an EPC7 List amplifier (filtered at 3 kHz) was stored on magnetic tape (Racal). The records were then analysed off-line; they were filtered with an 8-pole low-pass Bessel filter (cut-off frequency usually 1 kHz, and 2 kHz in the case of a few experiments on Na^+ currents), and digitized (with a sampling frequency 4 times higher than the filter frequency) for computer analysis (PDP 11–23). Note that the cascaded filters used give final cut-off frequencies close to 0·75 and 1·2 kHz.

Although we tried to use analog compensation of capacitive currents during the experiment, the compensation was generally not satisfactory because the access resistance to the cell interior had a tendency to increase continuously with time. This continuous drift often prevented the use of the series resistance compensation. At the beginning of the experiment, the series conductance value indicated by the analog compensation of the EPC7 List amplifier was generally between 0·15 and 0·3 μs. We terminated most experiments before this parameter became smaller than 0·1 μs. Since the recorded current rarely exceeded 500 pA, the voltage drop across the series resistance was usually smaller than 5 mV. Furthermore, possible kinetic changes in the voltage-dependent currents were checked systematically, and the experiments during which such changes occurred were discarded. The high reproducibility of the current–voltage (*I*–*V*) curves of the voltage-gated currents studied suggests that the errors due to the series resistance were small.

In view of the drift described above, we corrected the current recorded during a depolarizing voltage jump for both the leak and the residual capacitive currents by alternating between a depolarizing jump and a 20 mV 'control' voltage jump, which was either hyperpolarizing or depolarizing depending upon the difference between the holding potential and the threshold of the voltage-gated current. This procedure had the advantage of allowing us to take into account possible changes with time of both the leak and the capacitive currents. The voltage-jump duration was 50 ms and the frequency of the depolarizing voltage jumps never exceeded 0·5 Hz. During analysis, the current records obtained during successive identical voltage jumps were averaged and, assuming a linear leak, the average of the corresponding 'control' traces was multiplied by the appropriate factor and subtracted from the average of the current traces recorded during the test depolarization.

We have some evidence that the leak was indeed linear at least up to +30 mV and in some cases even above. In most experiments performed in the Na^+–0 Ca^{2+}–3 Mg^{2+}, Na^+–0 Ca^{2+}–1 Mg^{2+} and Na^+–0·5 Ca^{2+}–2·5 Mg^{2+} external solutions (see Figs 1, 2 and 3*A*), and in the few experiments performed in the presence of 5 mM-Co^{2+} (not shown), the current value measured at the end of a 50 ms duration voltage jump was linearly related to the membrane potential value. Furthermore, the leak was indeed linear in the voltage range where it was systematically measured below the threshold of the voltage-gated currents (from −87 to −27 mV in the experiments of Figs 4 and 5 and from −67 to −27 mV in the experiments of Figs 6 and 7*A* as indicated in each Figure by the zero value of the Ba^{2+} currents obtained at −27 mV after correction for a linear leak). Note that if, for very strong depolarizations, the leak became larger than assumed by the linear leak-subtraction procedure, we would have underestimated the amplitude of the sustained inward current activated by depolarization.

With the exception of the records shown in Fig. 3*B*, all the depolarization-activated inward currents illustrated have been corrected by the leak-subtraction procedure described above. However, in the isotonic Ba^{2+} solution, the Ba^{2+} currents were usually very large compared to the leak and could be detected even without leak subtraction (see legends of Figs 4–7). Note that since the number of averaged test or control traces was usually around four, the noise level of the depolarization-activated currents that have been illustrated is not representative of the noise actually induced by channel openings.

The cells used in most experiments were very flat; the diameter of their soma was often of the order of 70 μm and some of them showed long processes extending from their cell body. This geometry probably explains why a small delay was often observed between the onset of the depolarization and that of the voltage-gated currents. Consequently, we did not draw conclusions concerning detailed kinetic properties of these currents. In the younger, smaller round cells which were used in some experiments, the currents showed a more rapid onset and gave *I–V* curves similar to those illustrated. However, in these cells the currents were generally smaller and the sustained Ca^{2+} current was less frequently observed.

All the curves were drawn by eye.

RESULTS

K^+-free solutions

In the absence of external K^+ ions and in the presence of almost physiological external concentrations of Na^+, Ca^{2+} and Mg^{2+} ions (Na^+–2 Ca^{2+}–1 Mg^{2+} external solution), whole-cell current recordings revealed the existence of at least two types of inward currents activated by depolarization (Fig. 1). The initial current was a very brief transient one, that was not blocked by the substitution of external Ca^{2+} ions by Mg^{2+} (Fig. 1*A*) (but could be inactivated after suppression of Ca^{2+} ions if the holding potential was not negative enough: see Fig. 1*B* and Figure legend); this initial current appeared to be a TTX-sensitive, voltage-dependent Na^+ current (see Fig. 3). Depending upon the cell and the characteristics of the depolarizing jump, the later inward current appeared either to be transient (Fig. 1*A*) or to show a sustained component (Fig. 1*B*), but in both cases, it could be blocked by the suppression of

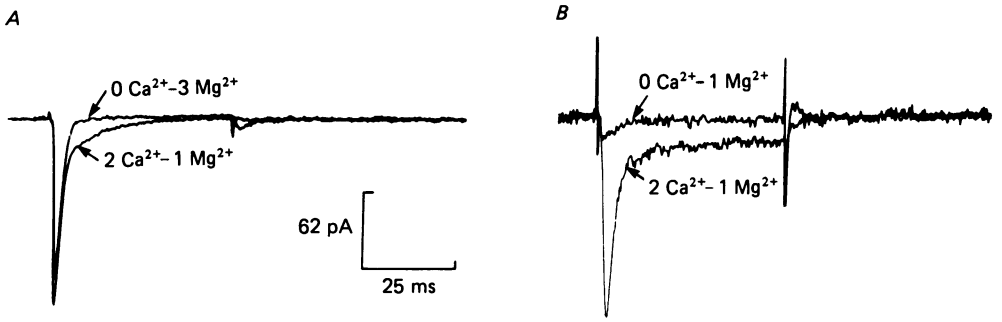

Fig. 1. Inward currents activated by depolarization in the Na^+–2 Ca^{2+}–1 Mg^{2+} solution. *A*, inward currents successively activated by depolarization from −107 to −12 mV in the Na^+–2 Ca^{2+}–1 Mg^{2+} and Na^+–0 Ca^{2+}–3 Mg^{2+} external solutions. In the Na^+–2 Ca^{2+}–1 Mg^{2+} solution, the depolarizing jumps activated two transient inward currents, an initial one which persisted in the 0 Ca^{2+} solution (and which was blocked by TTX (not shown)), and a second one, which could no longer be detected in the 0 Ca^{2+} solution. Note also the absence of sustained current at the end of the depolarizing jumps; this observation, which was done for even stronger depolarizations, indicates that the leak-subtraction procedure was satisfactory (see Methods). Whole-cell resistance below −60 mV: 2 GΩ in both solutions. *B*, inward currents successively activated by depolarization from −67 to −7 mV in another cell in the Na^+–2 Ca^{2+}–1 Mg^{2+} and Na^+–0 Ca^{2+}–1 Mg^{2+} external solutions. In the Na^+–2 Ca^{2+}–1 Mg^{2+} solution, the depolarizing jumps induced both an initial transient current (very similar to that illustrated in *A*) and a sustained inward current which was still detectable after a 50 ms depolarization. In the Na^+–0 Ca^{2+}–1 Mg^{2+} solution, the sustained current was no longer detected, which shows that the leak-subtraction procedure was correct, and indicates that this sustained current is a Ca^{2+} current. The apparent blockade of the initial inward current in the Na^+–0 Ca^{2+}–1 Mg^{2+} solution actually resulted from a shift towards more negative membrane potentials in the voltage dependence of the inactivation of this current (shift induced by the lowering of the external concentration of divalent cations); the initial inward current was still activated by depolarization in the Na^+–0 Ca^{2+}–1 Mg^{2+} solution, when the holding potential was made more negative (not shown). In this experiment, the capacitive currents were not completely suppressed by the usual subtraction procedure, because there was a too large drift of the series resistance. Whole-cell resistance below −60 mV: 5 and 3·3 GΩ in the presence and absence of Ca^{2+}.

external Ca^{2+} ions and persisted in the presence of 200 nM-TTX (see below); thus, whether transient or sustained, the later current appears to be carried by Ca^{2+} ions. As demonstrated below by the experiments performed with the isotonic Ba^{2+} solution, this current could be broken down into two distinct components, the relative amplitudes of which varied from cell to cell.

The Na^+ current

An external K^+-free solution containing only 0·5 mM-Ca^{2+} ions (the Na^+–0·5 Ca^{2+}–2·5 Mg^{2+} solution) was used in a few experiments in order to study the initial transient inward current while minimizing contamination by the two other depolarization-activated inward currents. As shown by Fig. 2*A* and *B*, the threshold of activation of the initial transient inward current was close to −45 mV (a result confirmed in four similar experiments). Very similar results were obtained in the

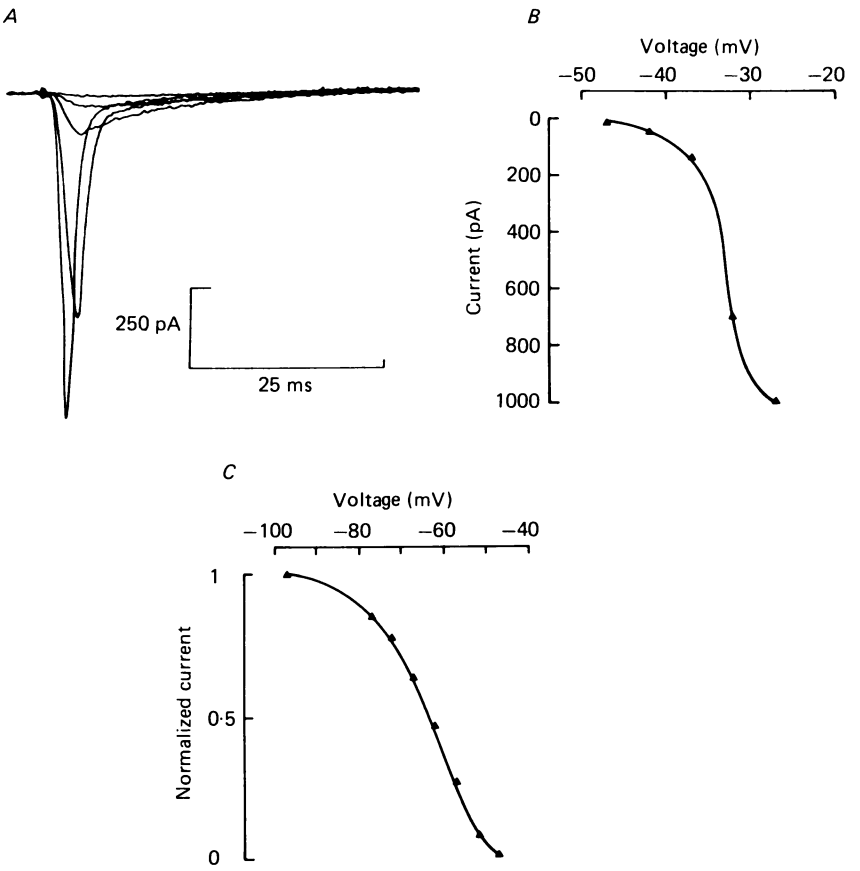

Fig. 2. Voltage-gated Na^+ current in the Na^+–0·5 Ca^{2+}–2·5 Mg^{2+} external solution. *A*, current activated by depolarizing jumps from −97 to −47, −42, −37, −32 and −27 mV. *B*, *I–V* curve of the peak inward current activated by depolarization in the experiment illustrated in *A*. *C*, voltage dependence of the steady-state inactivation of the Na^+ current of another cell. The cell was maintained at −97 mV between voltage jumps, and every 10 s, a 50 ms depolarizing jump to −17 mV was applied, either directly from −97 mV or at the end of 1 s pre-pulse to a variable membrane potential, *V*. The peak inward current activated at −17 mV by depolarization from the potential *V* is plotted as a function of *V*, after normalization with respect to its value in the absence of pre-pulse. Whole-cell resistance below −50 mV: 2·5 GΩ.

Na^+–2 Ca^{2+}–1 Mg^{2+} solution in three cells which did not show large Ca^{2+} currents, and in other experiments performed with K^+-containing solutions (see Fig. 8).

The voltage dependence of the steady-state inactivation of the Na^+ current is illustrated in Fig. 2*C*. The peak inward current activated by a test pulse to −17 mV was measured after a 1 s duration pre-pulse of variable amplitude. This current, normalized to its value in the absence of a pre-pulse, was plotted as a function of the pre-pulse membrane potential. In the two experiments in which such measurements were made, half-inactivation was observed around −65 mV.

As shown above, the initial transient inward current was not blocked by the

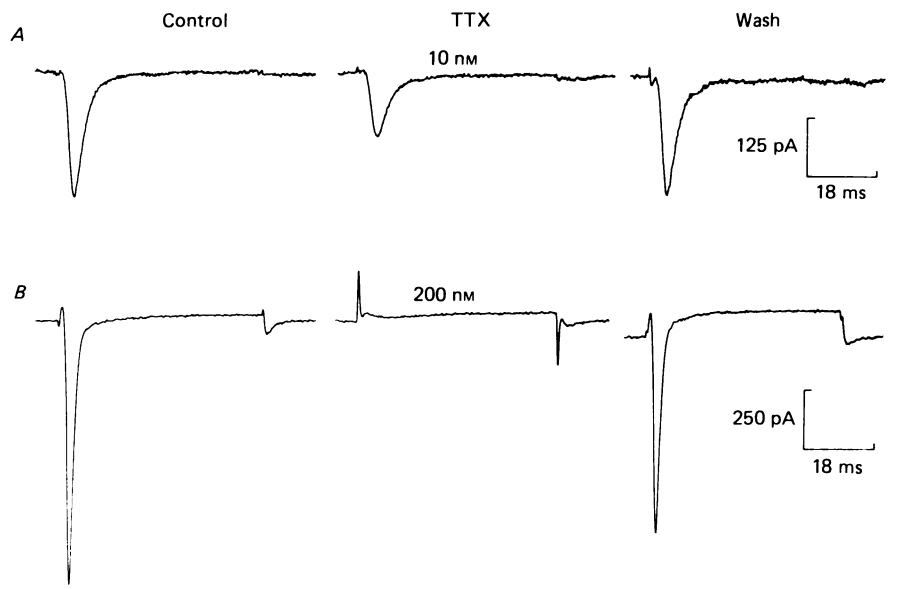

Fig. 3. TTX sensitivity of the initial transient inward current activated by depolarization in the Na^+–0·5 Ca^{2+}–2·5 Mg^{2+} external solution. *A*, half-blockade by 10 nM-TTX of the inward current activated by depolarization from −97 to −17 mV. Whole-cell resistance below −50 mV: 2·5 GΩ. *B*, complete blockade by 200 nM-TTX of the inward current activated in another cell by depolarization from −97 to −27 mV. In this case, the current traces which are illustrated are the original ones, uncorrected for the leak current (it is evident that the cell deteriorated slightly during wash); the capacitive transients were roughly compensated before the recording, but have not been corrected by the usual subtraction procedure.

external Ca^{2+}–Mg^{2+} substitution; neither was it blocked by addition of 5 mM-Co^{2+} to the external Na^+–2 Ca^{2+}–1 Mg^{2+} solution. However, it was completely blocked by the substitution of external Na^+ ions by Tris or *N*-methyl glucamine (not illustrated). Furthermore, this current was TTX (tetrodotoxin) sensitive. It was reduced by half in solutions containing 10 nM-TTX (Fig. 3*A*) and was completely blocked by 200 nM-TTX (Fig. 3*B*). The complete blockade of this current by 200 nM-TTX was observed in ten experiments.

These results clearly show that the initial transient inward current is a classical TTX-sensitive voltage-gated Na^+ current.

The Ca^{2+} currents

Voltage-dependence in the isotonic Ba^{2+} solution. The isotonic Ba^{2+} solution was used in order to enhance the current flowing through Ca^{2+} channels and to prevent intracellular Ca^{2+} accumulation (known to induce inactivation of sustained Ca^{2+} currents in other cell types) (see also Methods). As shown below, in most osteoblasts, two Ba^{2+} currents were detectable: a transient one and a sustained one. However, their relative amplitude varied greatly among cells (see Discussion). We shall first describe the extreme cases, in which one of these two currents is clearly predominant.

Figure 4*A* illustrates the case in which the predominant Ba^{2+} current is the

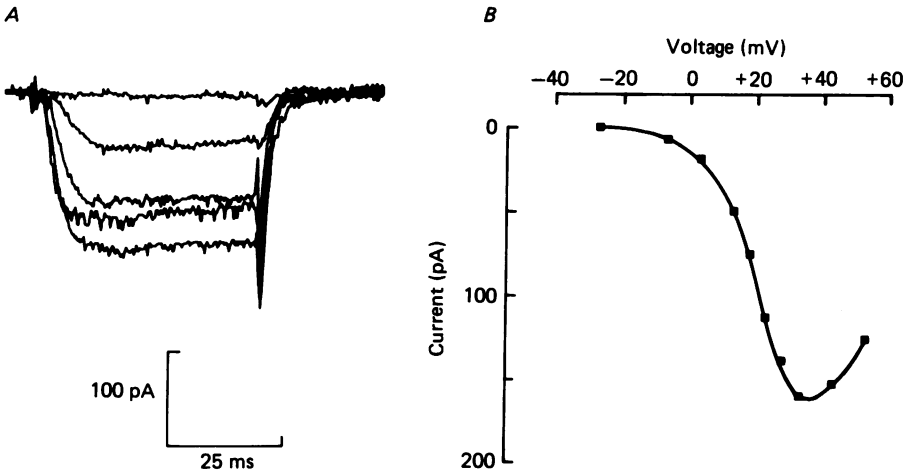

Fig. 4. Voltage dependence of the sustained inward current activated by depolarization in the isotonic Ba^{2+} solution. *A*, inward currents activated by depolarizing jumps from −67 to −7, +13, +23, +33 or +53 mV. *B*, *I–V* curve of the sustained Ba^{2+} current in the experiment illustrated in *A*. The current value which is plotted is the current measured at the end of each depolarization (after correction for the leak current). In this experiment, the transient Ba^{2+} current was less than 20% of the total depolarization-activated Ba^{2+} current (estimation obtained from the decrease of the depolarization-activated inward current during depolarizations around +10 mV). Up to +40 mV, the sustained Ba^{2+} current increases with depolarization although the driving force for Ba^{2+} ions decreases; above +40 mV, the sustained Ba^{2+} current decreases with depolarization. Generally, above +60 mV, the Ba^{2+} currents could no longer be measured precisely because of the slow activation of an outward current. The whole-cell resistance corresponding to the linear leak observed below −20 mV was 6·7 GΩ. Thus, for the maximum Ba^{2+} current of 160 pA (obtained here with a 100 mV voltage jump), the change in leak current would be only 15 pA.

sustained Ba^{2+} current. In five such cells, *I–V* curves of the sustained Ba^{2+} current were obtained using a holding potential of −67 mV, by measuring the current activated by depolarization at the end of each voltage jump (Fig. 4*B*). The sustained Ba^{2+} current reaches its maximum at about +40 mV.

Figure 5*A* illustrates the case in which the predominant Ba^{2+} current is the *transient* Ba^{2+} current. Above 0 mV, the inward current remaining at the end of a given depolarization was only a small fraction of the peak current activated by this depolarization ($\frac{1}{10}$ at +3 and +13 mV, $\frac{1}{7}$ at +23 mV). Thus, in this cell, the peak inward current activated by depolarization to around +10 mV was only slightly contaminated by the sustained Ba^{2+} current. Figure 5*B* shows the *I–V* curve of this peak current. It is clear that the transient Ba^{2+} current reaches a maximum at about +10 mV. This result was confirmed in six similar experiments performed in cells showing a predominant transient Ba^{2+} current, and in four experiments in which two series of depolarizing voltage jumps were successively applied from two different holding potentials (−87 or −67 and −32 or −27 mV) (see below). Thus, the membrane potential corresponding to the maximum *transient* Ba^{2+} current is about 30 mV less depolarized than the membrane potential corresponding to the maximum *sustained* Ba^{2+} current.

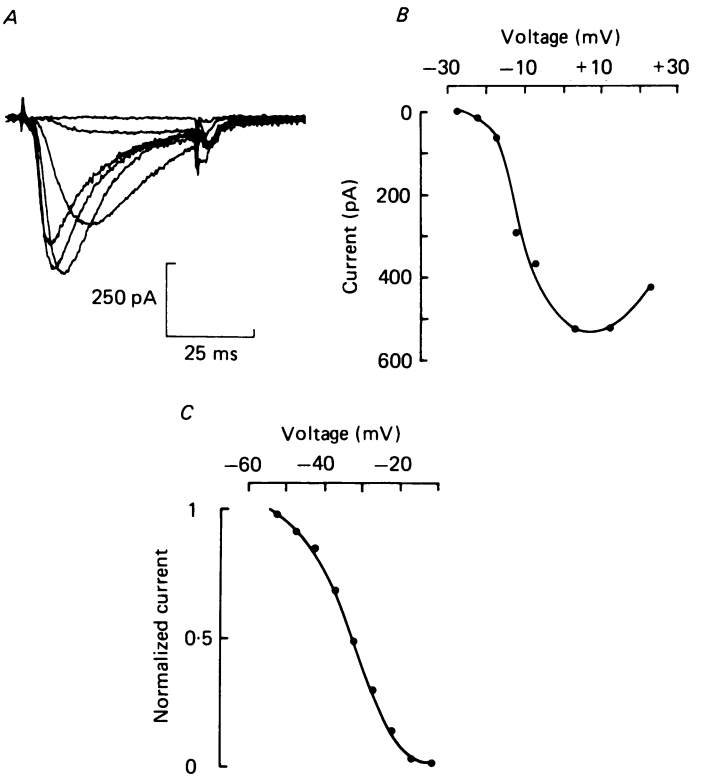

Fig. 5. Voltage dependence of the transient Ba^{2+} current activated by depolarization in the isotonic Ba^{2+} solution containing 200 nM-TTX. *A*, inward currents activated by depolarization from −67 to −27, −17, −7, +3, +13 and +23 mV in a cell showing a predominant transient Ba^{2+} current (see text). Although the records have been corrected by the usual subtraction procedure, small capacitive currents are still visible; furthermore, there is an apparent delay between the onset of the depolarization and the onset of the current, which is not observed in all cells and is probably artifactual (see Methods). *B*, *I–V* curve of the peak Ba^{2+} current recorded in the experiment illustrated in *A*. As found in all the cells showing a transient Ba^{2+} current, the threshold of the Ba^{2+} current which is activated by depolarization in this experiment was close to −25 mV and the maximum value of the transient Ba^{2+} current was observed at about +10 mV. The whole-cell resistance corresponding to the linear leak observed below −20 mV was 3·6 GΩ. Thus, for the maximum Ba^{2+} current of 550 pA (obtained here with a 70 mV voltage jump) the change in leak current would be only 20 pA. *C*, voltage dependence of the steady-state inactivation of the transient Ba^{2+} current (same cell as in *A* and *B*). Between voltage jumps, the cell was held at −67 mV, and every 10 s, a 50 ms depolarizing jump to +3 mV was applied either directly from −67 mV or at the end of a 1 s pre-pulse to a variable membrane potential, *V*. The peak inward current activated at +3 mV by depolarization from the potential *V* is plotted as a function of *V*, after normalization with respect to its value in the absence of pre-pulse.

Because of the difference in time course of the two Ba^{2+} currents present during strong depolarizations, they have been labelled the 'transient' and 'sustained' Ba^{2+} currents respectively. However, even in cells in which the 'transient' inward current is dominant during a strong depolarizing jump, that same current type activated by a small depolarizing jump (one close to the threshold of activation of the total Ba^{2+}

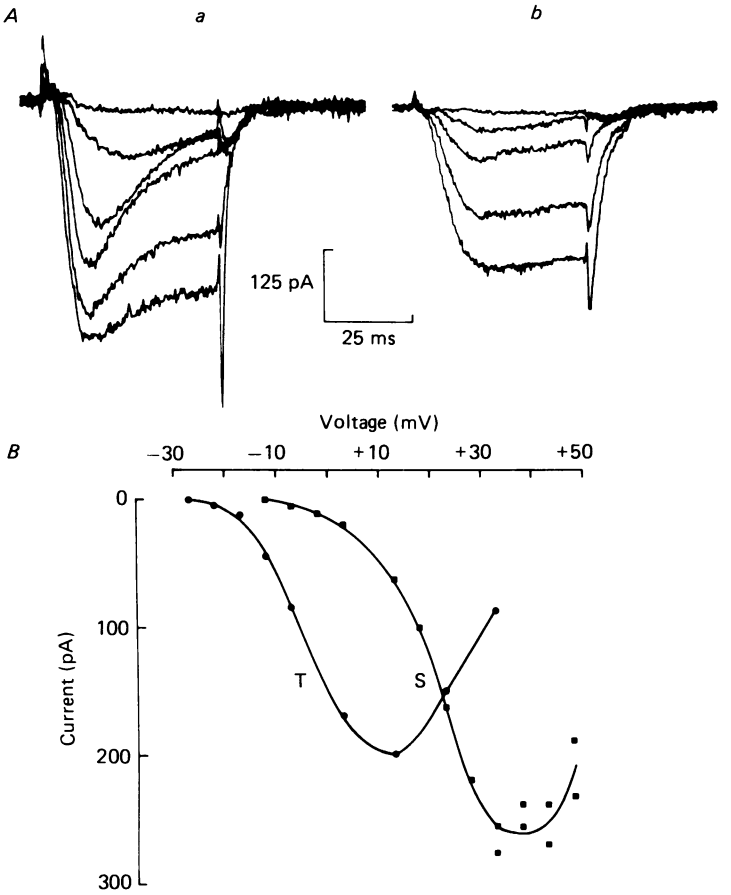

Fig. 6. Comparison of the voltage dependence of the two Ba^{2+} currents in a given cell. *A*, inward currents activated by depolarization in the isotonic Ba^{2+} solution containing 200 nM-TTX, first during voltage jumps from −67 towards −17, −7, +3, +13, +23 and +33 mV (*a*) and then, after changing the holding potential, during voltage jumps from −27 towards −7, +3, +13, +23 and +33 mV (*b*). In *a*, both a transient Ba^{2+} current and a sustained Ba^{2+} current are detected whereas in *b*, the transient component is markedly reduced. (The sustained component is also slightly reduced, which might result directly from the holding potential change, but is likely to result from a slight 'run-down' over time of the sustained Ba^{2+} current.) *B*, *I–V* curves of the transient (T,●) and sustained (S,■) Ba^{2+} currents in the experiment illustrated in *A*. The sustained current was measured from the records obtained from −27 mV, either at the end of the depolarizing jumps (up to +30 mV), or both at the end of the depolarizing jumps and at the maximum of the depolarization-activated inward current (above +30 mV). Indeed, for membrane potentials more depolarized than +30 mV, the current measured at the end of the depolarization seemed to be slightly contaminated by a depolarization-activated outward current which became larger with stronger depolarizations. The transient Ba^{2+} current was estimated, above −7 mV, as the difference between the maximum and final values of the depolarization-activated inward current, and below −7 mV, as the maximum depolarization-activated inward current. At −7 mV, it was estimated as the difference between the maximum inward current activated from −67 mV and the sustained inward current activated from −27 mV. Whole-cell resistance below −20 mV: 1·6 GΩ.

current) looks like a 'sustained' current during the 50 ms duration of the depolarization (see the record obtained at −17 mV in the experiment illustrated by Fig. 5). Note that this observation has also been made in other cell types (see for example Fig. 12 in Carbone & Lux, 1987). Thus, the evaluation of the relative contributions of the two Ba^{2+} currents close to the threshold of activation of the total Ba^{2+} current requires a specific blockade of one of these two currents (see below Fig. 6).

The voltage dependence of the steady-state inactivation of the transient Ba^{2+} current is illustrated in Fig. 5*C*. The peak inward current activated by a test pulse to +3 mV was measured after a 1 s duration pre-pulse of variable amplitude. (Note that in this cell, at +3 mV, the sustained Ba^{2+} current represents at most 10% of the peak current.) The transient current, normalized to its value in the absence of a pre-pulse is plotted as a function of the pre-pulse membrane potential. It decreases as the pre-pulse amplitude increases. In five similar experiments, half-inactivation was observed at about −35 mV. In two of these experiments, very similar steady-state inactivation curves were obtained with pre-pulses of either 1 or 10 s duration.

In order to determine the contributions of each of the two Ba^{2+} currents in cells in which these two currents seem to have similar amplitudes, we took advantage of the possibility of inactivating the transient current by depolarization. The currents obtained using two different holding potentials were compared. Such an experiment is illustrated by Fig. 6. The records shown in Fig. 6*Aa* were obtained by applying depolarizing jumps from a holding potential of −67 mV; the inward current activated during these voltage jumps was clearly a mixture of sustained current and transient current (the transient current was particularly large around +10 mV). The records shown in Fig. 6*Ab* were obtained from the same cell during depolarizing jumps from −27 mV; this holding potential strongly inactivated the transient Ba^{2+} current so that the remaining inward current was predominantly a sustained Ba^{2+} current. (Note that in this case, the transient current was inactivated by about 83% by a holding potential of −27 mV (compare Fig. 6*Aa* and *b*), and that in the experiment of Fig. 5*C*, this degree of inactivation was induced by a pre-pulse to −23 mV; this small difference could result from a slight error in the estimate of the actual membrane potential and/or from the difference between the protocols used in these two experiments.)

In the experiment of Fig. 6, in order to completely inactivate the transient Ba^{2+} current, it would have been necessary to maintain the cell at a membrane potential even more depolarized than −27 mV (see Fig. 5*C*). However, this might have prevented a reliable measurement of the threshold of activation of the sustained Ba^{2+} current. Thus, we rather held the cell at −27 mV and measured the sustained current at the end of the depolarizing jumps.

The *I–V* curve thus obtained shows that in the isotonic Ba^{2+} solution the threshold of activation of the sustained inward current is close to −10 mV (a result confirmed in three other similar experiments), whereas this current is maximal at around +40 mV (as already shown by using depolarizing jumps from a more negative membrane potential, in cells showing a predominant sustained Ba^{2+} current (see Fig. 4)).

The *I–V* curve of the transient Ba^{2+} current was obtained from the current traces

during depolarizing jumps from −67 mV (Fig. 6*B* (●)). Above 0 mV, the transient Ba^{2+} current was measured as the difference between the maximum and final values of the depolarization-activated inward current. This current was maximal around +10 mV. Below −10 mV (threshold of activation of the sustained Ba^{2+} current), the transient Ba^{2+} current is identical to the total inward current activated from −67 mV.

Note that because of the high threshold of the sustained Ba^{2+} current, the threshold of activation of the transient Ba^{2+} current is the threshold of activation of the total Ba^{2+} current. In the isotonic Ba^{2+} solution, this threshold was always close to −25 mV (more than ten experiments).

In summary, the 'sustained' and 'transient' currents could also be named the 'high-threshold' and 'low-threshold' currents. In order to reach the threshold or the maximum of the current, it is necessary to apply larger depolarizations in the case of the sustained current than in the case of the transient current. Thus, osteoblasts show two different kinds of voltage-gated Ca^{2+} currents, which differ by their time course, by their sensitivity to depolarizing pre-pulses and by the voltage dependence of their activation curve.

Preliminary experiments indicate that the total Ca^{2+} current of osteoblasts is sensitive to both Bay K8644 (Schramm, Thomas, Towart & Franckowiak, 1983) and (+)-PN 200-110 (Hof, Hof, Ruegg, Cook & Vogel, 1986). In three experiments performed in the isotonic Ba^{2+} solution, 50 nM-Bay K8644 strongly enhanced the Ba^{2+} current measured at the end of a depolarizing jump from −67 to +3 mV (by a factor of 16, 9 and 15). In three other experiments, also performed in the isotonic Ba^{2+} solution, 10 nM-(+)-PN 200-110 reduced by a factor of about 4 (4·2, 3·6 and 4·2) the Ba^{2+} current measured at the end of a depolarizing jump from −67 to +33 mV; this effect was half-reversible after a few minutes wash.

Physiological concentrations of external divalent cations. The two TTX-insensitive inward currents activated by depolarization could also be observed in the Na^+–2 Ca^{2+}–1 Mg^{2+} external solution (see Fig. 1). In the experiment illustrated in Fig. 7*A*, the sustained current activated by depolarization was very large in the isotonic Ba^{2+} solution; thus it could be clearly detected in the Na^+–2 Ca^{2+}–1 Mg^{2+} external solution, although its maximum value was about 15 times smaller than in the isotonic Ba^{2+} solution. Note that a small transient current was also present in this cell. *I–V* curves for the sustained Ba^{2+} current measured in the same cell in the isotonic Ba^{2+} solution and in the Na^+–2 Ca^{2+}–1 Mg^{2+} solution are shown in Fig. 7*C*. Replacing the isotonic Ba^{2+} solution by physiological concentrations of Na^+, Ca^{2+} and Mg^{2+} shifted the *I–V* curve of the sustained current by about 30 mV towards less-depolarized membrane potentials. In the Na^+–2 Ca^{2+}–1 Mg^{2+} solution, the maximum value of the sustained Ca^{2+} current was reached at about +10 mV.

In the experiment illustrated in Fig. 7*B*, the transient current was larger than the sustained current in the isotonic Ba^{2+} solution, and was clearly the predominant current in the Na^+–2 Ca^{2+}–1 Mg^{2+} solution. Note that the transient current of Fig. 7*B* was much less reduced than the sustained current of Fig. 7*A* by the substitution of the isotonic Ba^{2+} solution by the Na^+–2 Ca^{2+}–1 Mg^{2+} solution.

The activation and steady-state inactivation curves of the transient current recorded in the Na^+–2 Ca^{2+}–1 Mg^{2+} solution in the experiment of Fig. 7*B* are

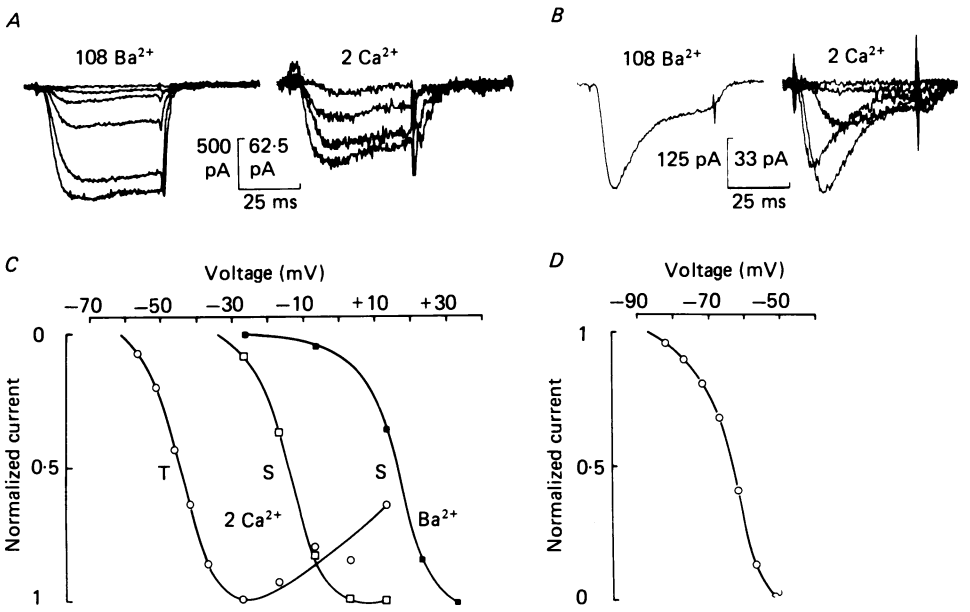

Fig. 7. Sustained (S, *A* and *C*) and transient (T, *B*, *C* and *D*) currents activated by depolarization in the Na^+–2 Ca^{2+}–1 Mg^{2+} solution. Comparison with the currents recorded in the isotonic Ba^{2+} solution. TTX (200 nM) was present in both solutions. *A*, sustained currents activated in a given cell by depolarization from −67 to −27, −7, +3, +13, +23 and +33 mV in the Ba^{2+} solution (left records) and by depolarization from −87 to −37, −17, −7 and +13 mV in the Na^+–2 Ca^{2+}–1 Mg^{2+} solution (right records). Note the unusually large amplitude of the sustained Ba^{2+} current (maximum value close to 1 nA). In the isotonic Ba^{2+} solution, the whole-cell resistance corresponding to the linear leak observed below −20 mV was 1·6 GΩ. Thus, for the maximum Ba^{2+} current of 1000 pA (obtained here with a 100 mV voltage jump), the change in leak current would be only 60 pA. In the Na^+–2 Ca^{2+}–1 Mg^{2+} solution, the whole-cell resistance measured below −40 mV was 1 GΩ. *B*, transient currents activated in another cell by depolarization from −97 to +13 mV in the isotonic Ba^{2+} solution (left record) and by depolarization from −97 to −67, −57, −47, −27 and −7 mV in the Na^+–2 Ca^{2+}–1 Mg^{2+} solution (right records). In the isotonic Ba^{2+} solution, the whole-cell resistance corresponding to the linear leak observed below −20 mV was 3·2 GΩ. Thus, for the maximum Ba^{2+} current of 200 pA (obtained here with a 110 mV voltage jump), the change in leak current would be only 34 pA. In the Na^+–2 Ca^{2+}–1 Mg^{2+} solution, the whole-cell resistance measured below −60 mV was 2·1 GΩ. *C*, *I–V* curves of the sustained inward current (measured at the end of the depolarizing jumps) in the isotonic Ba^{2+} (■) and Na^+–2 Ca^{2+}–1 Mg^{2+} (□) solutions, in the experiment illustrated in *A*; *I–V* curve of the peak inward current recorded in the Na^+–2 Ca^{2+}–1 Mg^{2+} solution in the experiment illustrated in *B* (○). Note the shift induced by the substitution of the isotonic Ba^{2+} solution by the Na^+–2 Ca^{2+}–1 Mg^{2+} solution, and the difference in activation voltage range between the two types of Ca^{2+} currents observed in the Na^+–2 Ca^{2+}–1 Mg^{2+} solution. *D*, voltage dependence of the steady-state inactivation of the transient Ca^{2+} current recorded in the Na^+–2 Ca^{2+}–1 Mg^{2+} solution, in the experiment illustrated in *B* (holding potential −97 mV, test pulse to −27 mV; see the method described in Fig. 5 legend).

illustrated in Fig. 7*C* (○) and *D*. When compared to the curves obtained in the isotonic Ba^{2+} solution (see Fig. 5), both the activation curve and the steady-state inactivation curve appear to be shifted towards less-depolarized membrane potentials (by 30–35 mV). In the Na^+–2 Ca^{2+}–1 Mg^{2+} solution, the threshold and the maximum of the transient current were reached at about −60 and −25 mV respectively; half-inactivation was observed around −65 mV.

Internal pCa 7. The internal solution used in all the above experiments was buffered at pCa 8. This choice was made in order to facilitate the detection of voltage-gated Ca^{2+} currents since it is known that the sustained Ca^{2+} current of most cell types is particularly sensitive to the internal Ca^{2+} concentration (see Eckert & Chad, 1984). However, experiments using the Ca^{2+} indicator quin-2 have suggested that the physiological concentration of intracellular Ca^{2+} in osteoblasts is of the order of 10^{-7} M (Löwik *et al.* 1985). We thus performed a few experiments using the isotonic Ba^{2+} solution and the internal Cs–HEDTA solution buffered at pCa 7 (see Methods). In these experiments, the transient Ba^{2+} current was always observed and its activation and steady-state inactivation curves were very similar to those presented above. The sustained Ba^{2+} current was still present but was more difficult to detect than with the Cs–EGTA internal solution. (In a cell showing a pure sustained current, the threshold and the maximum amplitude (330 pA) of this current were reached respectively at about −10 and +40 mV, as was usually found with the Cs–EGTA internal solution.)

Physiological solutions

The results presented above were all obtained in the absence of internal and external K^+ ions. A few experiments were performed using the Na^+–2 Ca^{2+}–1 Mg^{2+}–5 K^+ external solution and the K–HEDTA internal solution buffered at pCa 7, in order to know whether, in the presence of physiological concentrations of K^+ ions, the depolarization-activated inward currents would still represent an appreciable fraction of the total current and could give rise to regenerative depolarizations similar to the action potentials of excitable cells.

Under voltage clamp, the depolarization-activated Na^+ and Ca^{2+} currents could still be detected and, up to −10 mV, these Na^+ and Ca^{2+} currents represented in at least some cells a large fraction of the total current (Fig. 8*A*). The Na^+ current could be estimated by the difference between the current records obtained successively in the absence and presence of 200 nM-TTX, whereas the peak Ca^{2+} current was measured in the presence of TTX; the *I–V* curves of these two currents are plotted in Fig. 8*B*. With the physiological solutions used in this experiment the threshold of activation of the Na^+ current was close to −45 mV; the threshold of activation of the total Ca^{2+} current (which seems to be mostly a transient Ca^{2+} current) was close to −60 mV and its maximum value was reached at about −25 mV. These results agree with those which were obtained from experiments performed with the K^+-free Na^+–2 Ca^{2+}–1 Mg^{2+} external solution and the Cs–EGTA internal solution (see above).

Under current clamp, it was possible to induce action potentials in osteoblasts (Fig. 8*C*). Similar regenerative depolarizations could also be observed in the presence of 200 nM-TTX (not shown).

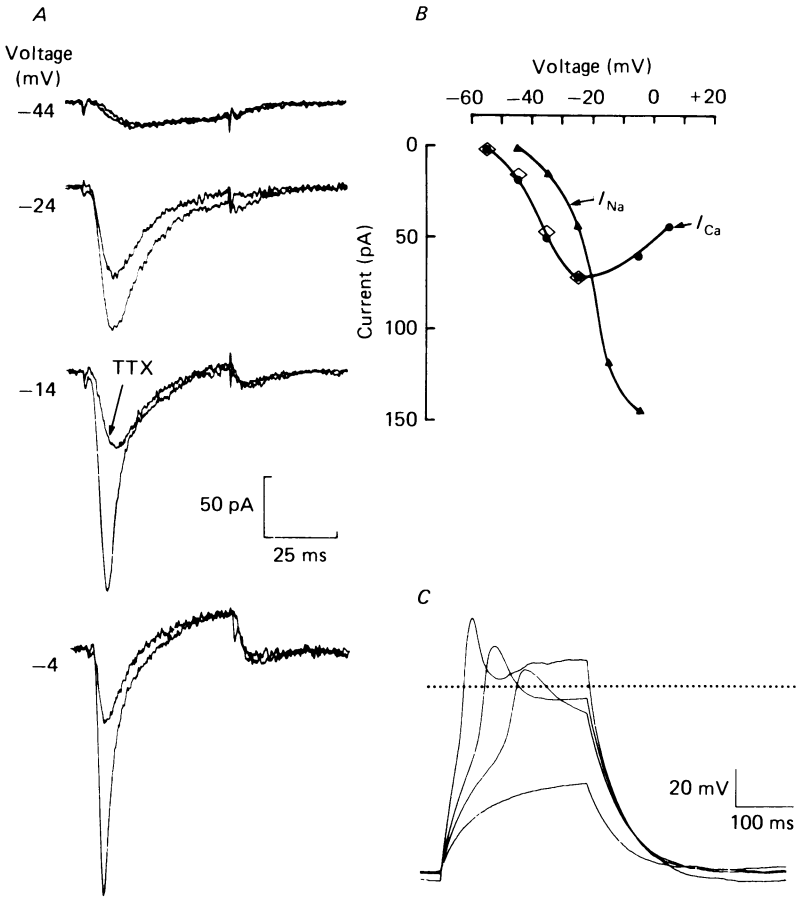

Fig. 8. Voltage-clamp and current-clamp records obtained with physiological solutions (Na^+–5 K^+–2 Ca^{2+}–1 Mg^{2+} external solution, K–HEDTA internal solution). *A*, currents activated by depolarization from −84 to −44, −24, −14 or −4 mV; for each of these depolarizations, the current traces successively obtained from the same cell in the absence and presence of 200 nM-TTX are superimposed. Note that it is only above −10 mV that an outward current is detectable at the end of the depolarizing jump. In the absence of TTX, at −4 mV, the amplitude of this outward current is only 15% of that of the peak inward current (in the presence of TTX, it is only 50% of the peak inward current). Whole-cell resistance below −60 mV of about 2·4 GΩ in the presence or absence of TTX. *B*, *I–V* curves of the peak Ca^{2+} current (I_{Ca}) measured in the presence of TTX in the experiment illustrated in *A* (●) and of the Na^+ current (I_{Na}) of the same cell, which was estimated by taking the difference between the records obtained in the absence and presence of TTX (▲). The open lozenges (◇) indicate the *I–V* curve of the peak inward current which was activated by depolarization from −84 mV in the absence of TTX in another cell (when using voltage clamp in the experiment illustrated in *C*). This curve has been normalized with respect to the current value obtained at −24 mV (147 pA in this cell, 72 pA in the cell illustrated in *A*), so that the current scale is correct only for the *I–V* curves of the experiment illustrated in *A*. *C*, voltage traces obtained in current clamp in the absence of TTX during depolarizing current pulses of 500 ms duration and various amplitudes (20, 30, 40 and 70 pA). 0 mV is indicated by the dotted line. Strong current pulses were able to induce action potentials, the threshold of which seems to be close to −45 mV. In this cell voltage-clamp records were also obtained during depolarizing voltage jumps from −84 up to −24 mV and showed mostly Ca^{2+} currents (see *B* (◇)). Whole-cell resistance below −60 mV: 1·5 GΩ.

DISCUSSION

We have shown the existence of three kinds of depolarization-activated inward currents in osteoblasts from newborn rat calvaria: a TTX-sensitive Na^+ current and two different kinds of voltage-gated Ca^{2+} currents.

Na^+ current

Voltage-gated Na^+ channels have been most thoroughly studied in nerve and muscle cells and were traditionally considered as specific for these 'excitable' cells. In such cells, at least two kinds of depolarization-activated Na^+ channels, showing different TTX sensitivities, have been described. Na^+ currents that are much less sensitive to TTX than are the classical TTX-sensitive Na^+ channels (Narahashi, 1974) have been described in cardiac cells (see for example Cohen, Bean, Colatsky & Tsien, 1981), neurones (see Gallego, 1983 and Bossu & Feltz, 1984), or skeletal muscle cells at certain stages of their development (see Weiss & Horn, 1986 and included references). Biochemical data also indicate the existence of several classes of Na^+ channels (see Barchi, 1987 for a review). The affinity for TTX of 'TTX-sensitive' Na^+ channels corresponds to a K_d (dissociation constant) of a few nanomoles whereas that of the 'TTX-resistant' Na^+ channels corresponds to a K_d of about 1 μM. Voltage-gated Na^+ currents have also been detected in other cell types such as Schwann cells (Chiu, Schrager & Ritchie, 1984), glial cells (Nowak, Ascher, Berwald-Netter & Couraud, 1983; Bevan, Chiu, Gray & Ritchie, 1985; Nowak, Ascher & Berwald-Netter, 1987) and lymphocytes (rarely in human peripheral T lymphocytes or thymocytes (Cahalan, Chandy, DeCoursey & Gupta, 1985; Schlichter, Sidell & Hagiwara, 1986*a*), more frequently in murine T lymphocytes or in some human cell lines (DeCoursey, Chandy, Gupta & Cahalan, 1985; Schlichter, Sidell & Hagiwara, 1986*b*; DeCoursey, Chandy, Gupta & Cahalan, 1987)). A voltage-gated Na^+ current responsible for regenerative depolarizations has also been detected in fibroblasts, but only in the presence of veratridine (Frelin, Lombet, Vigne, Romey & Lazdunski, 1982). While the TTX sensitivity of the Na^+ currents found in glial cells is rather low (half-blockade requires 400–500 nM-TTX (Bevan *et al.* 1985; Nowak *et al.* 1987)), the Na^+ current of Schwann cells (Chiu *et al.* 1984), the Na^+ current occasionally found in human peripheral T lymphocytes (Cahalan *et al.* 1985) and the Na^+ current found in an erythroleukemic cell line (Schlichter *et al.* 1986*b*) are highly TTX sensitive. The voltage-gated Na^+ current found in osteoblasts, which is half-blocked by 10 nM-TTX and almost completely blocked by 200 nM-TTX, is a highly TTX-sensitive Na^+ current. Its threshold of activation is close to -45 mV, that is closer to the threshold of the Na^+ current of Schwann cells than to the threshold of the Na^+ current of the Ranvier node (Shrager, Chiu & Ritchie, 1985).

Ca^{2+} currents

Voltage-gated Ca^{2+} currents have been described not only in classical excitable cells but also in other cell types including several types of secretory cells (see Hagiwara & Byerly, 1981). More recently, the existence of at least one kind of voltage-gated Ca^{2+} current was also shown in myeloma or hybridoma secreting immunoglobulins (Fukushima & Hagiwara, 1983; Fukushima, Hagiwara & Saxton,

1984), in spermatogenic cells (Hagiwara & Kawa, 1984) and in glial cells (MacVicar, 1984; Newman, 1985).

In the present study, it was shown that in osteoblasts, depolarizing jumps induce voltage-gated Ca^{2+} currents in addition to a Na^+ current. Voltage-gated Ca^{2+} currents could be detected in the presence of 2 mM-external Ca^{2+} ions (Figs 1, 7 and 8) but were more easily studied in the isotonic Ba^{2+} solution. Using this solution and 200 nM-TTX, two different kinds of voltage-gated Ba^{2+} currents could be clearly observed, with much larger amplitudes than the leak, and without any intracellular Ca^{2+} accumulation. These currents differed strikingly from each other by their time course, voltage dependence of activation and steady-state inactivation. One is a sustained current, with a maximum around +40 mV, the other is a transient inactivating current, with a maximum around +10 mV. The relative proportions of these two currents varied greatly among cells, which facilitated the study of each of them.

In some cells, the current flowing through Ca^{2+} channels was predominantly a sustained current (Figs 4 and 7*A*), whereas in other cells, it was primarily a transient current (Fig. 5). However, in most cells, both a transient component and a sustained component were clearly present (Fig. 6).

In cells showing comparable transient and sustained depolarization-activated Ba^{2+} currents, the sustained component could be isolated by using a depolarizing holding potential which inactivated the transient component. By comparing the *I–V* curves of the depolarization-activated inward currents obtained in such cells from two different holding potentials, it was established that the threshold of activation of the transient current is more negative (by at least 15 mV) than the threshold of activation of the sustained current (Fig. 6); this result agrees with those obtained from cells showing a predominance of one of the two Ba^{2+} currents. Thus, the transient Ba^{2+} current observed in osteoblasts was more similar to the 'T' (or 'SD') current observed in many other cell types (Nilius, Hess, Lansman & Tsien, 1985; Bean, 1985 (cardiac cells); Armstrong & Matteson, 1985; Matteson & Armstrong, 1986 (pituitary cells); Cognard, Lazdunski & Romey, 1986; Beam, Knudson & Powell, 1986 (skeletal muscle cells); Carbone & Lux, 1986; and Miller, 1985 (reviews concerning neurones)) than to the 'N' current, thus far only detected in neurones (Nowycky, Fox & Tsien, 1985).

A variability in the amplitude of Ca^{2+} currents has already been reported in the case of several other cell types including cell lines (Fukushima *et al.* 1984; Matteson & Armstrong, 1986; Narahashi, Tsunoo & Yoshii, 1987) and primary cultures (Cota, 1986 (adult rat pituitary cells); Yaari, Hamon & Lux, 1987 (embryonic rat hippocampal neurones)). In the two latter studies, it has been shown that the ratio of the sustained current amplitude over the transient current amplitude increases with the age of the culture. In the present study we saw the same tendency when comparing the results obtained on day 3 and day 5 after plating, but some variability existed even within a given culture dish. The variability in the amplitude of Ca^{2+} currents is usually considered as being related either to the phase of the cell cycle or to the state of differentiation of the cell. The understanding of this variability would obviously require further studies.

As reported above, in the isotonic Ba^{2+} solution, the threshold of activation and

the maximum value of the Ca^{2+} currents of osteoblasts were reached respectively at about -25 and $+10$ mV for the transient current, and at about -10 and $+40$ mV for the sustained current. In external solutions containing physiological concentrations of divalent cations, the I–V curves of these currents are clearly shifted towards more negative membrane potentials (see also, for example, Carbone & Lux, 1987); the maximum of the sustained current is reached at about $+10$ mV (Fig. 7), whereas the threshold of activation and the maximum value of the transient current are reached respectively at about -60 and -25 mV (Figs 7 and 8). Thus, these currents might be activated under physiological conditions. Note, however, that in order for the transient current to be activated during a depolarizing stimulus, the membrane potential would first have to be lower than -50 mV, in order to avoid complete inactivation. Sufficiently negative resting potentials have already been observed in osteoblasts (Edelman, Fritsch & Balsan, 1986).

Our results suggest that under certain conditions, osteoblasts can produce action potentials. The regenerative depolarizations that we have observed were due most probably to the activation of Ca^{2+} (rather than Na^+) currents (being observed in the presence of 200 nM-TTX, and in cells showing only a small Na^+ current).

It has been shown previously that osteoblasts can be depolarized by PTH (Edelman *et al.* 1986). Although the precise mechanism responsible for this PTH response remains to be determined, it seems possible that the PTH-induced depolarization leads to a Ca^{2+} entry through the voltage-gated Ca^{2+} channels carrying the currents described in the present paper. This would be in agreement with the observation that PTH can stimulate Ca^{2+} influx and can increase, at least transiently, the intracellular Ca^{2+} concentration in osteoblasts (Löwick *et al.* 1985).

In osteoblasts as in other cell types, Ca^{2+} influx through voltage-gated Ca^{2+} channels could affect both contraction and secretion.

The osteoblasts which line the bone matrix in a continuous cell layer retract in response to PTH (Jones & Boyde, 1976; Jones & Ness, 1977); this effect is supposed to facilitate the degradation of the matrix by exposing the bone surface to the action of osteoclasts.

Furthermore, osteoblasts might be considered as 'secretory cells'. PTH rapidly induces the liberation of collagenase from osteoblasts (Puzas & Brand, 1979; Sakamoto & Sakamoto, 1986), and a major intermediary between the PTH receptors present on osteoblasts and the activation of osteoclasts (a not yet completely identified factor) has been found recently in conditioned medium from PTH-treated osteoblasts (McSheehy & Chambers, 1986; Perry, Skogen, Chappel, Wilner, Kahn & Teitelbaum, 1987).

We are very grateful to P. Ascher and to S. Balsan for their continuing support and helpful discussions. We also wish to thank A. Edelman for having initiated this work and J. S. Kehoe for useful advice on the manuscript. This work was supported by the CNRS (UA 04-295, UA 04-583) and the Université Pierre et Marie Curie.

REFERENCES

ARMSTRONG, C. M. & MATTESON, D. R. (1985). Two distinct populations of calcium channels in a clonal line of pituitary cells. *Science* **227**, 65–67.

BARCHI, R. L. (1987). Sodium channel diversity: subtle variations on a complex theme. *Trends in Neurosciences* **10** (6), 221–223.

BEAM, K. G., KNUDSON, C. M. & POWELL, J. A. (1986). A lethal mutation in mice eliminates the slow calcium current in skeletal muscle cells. *Nature* **320**, 168–170.

BEAN, B. P. (1985). Two kinds of calcium channels in canine atrial cells. *Journal of General Physiology* **86**, 1–30.

BEVAN, S., CHIU, S. Y., GRAY, P. T. A. & RITCHIE, J. M. (1985). The presence of voltage-gated sodium, potassium and chloride channels in rat cultured astrocytes. *Proceedings of the Royal Society* B **225**, 299–313.

BOLAND, C. J., FRIED, R. M. & TASHJIAN, A. H. (1986). Measurement of cytosolic free Ca concentrations in human and rat osteosarcoma cells: actions of bone resorption-stimulating hormones. *Endocrinology* **118**, 980–989.

BOSSU, J. L. & FELTZ, A. (1984). Patch-clamp study of the tetrodotoxin-resistant sodium current in group C sensory neurones. *Neuroscience Letters* **51**, 241–246.

BYERLY, L. & YAZEJIAN, B. (1986). Intracellular factors for the maintenance of calcium currents in perfused neurones from the snail, *Lymnea stagnalis*. *Journal of Physiology* **370**, 631–650.

CAHALAN, M. D., CHANDY, K. G., DECOURSEY, T. E. & GUPTA, S. (1985). A voltage-gated potassium channel in human T lymphocytes. *Journal of Physiology* **358**, 197–237.

CARBONE, E. & LUX, H. D. (1986). Low- and high-voltage-activated Ca channels in vertebrate cultured neurons: properties and functions. In *Experimental Brain Research*, vol. 14, ed. HEINEMANN, U., KLEE, M., NEHER, E. & SINGER, W., pp. 1–8. Heidelberg, Berlin: Springer-Verlag.

CARBONE, E. & LUX, H. D. (1987). Kinetics and selectivity of a low-voltage-activated calcium current in chick and rat sensory neurones. *Journal of Physiology* **386**, 547–570.

CHAMBERS, T. J. (1980). The cellular basis of bone resorption. *Clinical Orthopedics and Related Research* **151**, 283–293.

CHIU, S. Y., SCHRAGER, P. & RITCHIE, J. M. (1984). Neuronal-type Na and K channels in rabbit cultured Schwann cells. *Nature* **311**, 156–157.

COGNARD, C., LAZDUNSKI, M. & ROMEY, G. (1986). Different types of Ca^{2+} channels in mammalian skeletal muscle cells in culture. *Proceedings of the National Academy of Sciences of the U.S.A.* **83**, 517–521.

COHEN, C. J., BEAN, B. P., COLATSKY, T. J. & TSIEN, R. W. (1981). Tetrodotoxin block of sodium channels in rabbit Purkinje fibers. *Journal of General Physiology* **78**, 383–411.

COTA, G. (1986). Calcium channel currents in Pars Intermedia cells of the rat pituitary gland. *Journal of General Physiology* **88**, 83–105.

DECOURSEY, T. E., CHANDY, K. G., GUPTA, S. & CAHALAN, M. D. (1985). Voltage-dependent ion channels in T lymphocytes. *Journal of Neuroimmunology* **10**, 71–95.

DECOURSEY, T. E., CHANDY, K. G., GUPTA, S. & CAHALAN, M. D. (1987). Mitogen induction of ion channels in murine T lymphocytes. *Journal of General Physiology* **89**, 405–420.

DZIAK, R. & STERN, P. H. (1975). Calcium transport in isolated bone cells. III. Effects of parathyroid hormone and cyclic 3′,5′-AMP. *Endocrinology* **97**, 1281–1287.

ECKERT, R. & CHAD, J. D. (1984). Inactivation of Ca channels. *Progress in Biophysics and Molecular Biology* **44**, 215–267.

EDELMAN, A., FRITSCH, J. & BALSAN, S. (1986). Short-term effects of PTH on cultured rat osteoblasts: changes in membrane potential. *American Journal of Physiology* **251**, C483–490.

FENWICK, E., MARTY, A. & NEHER, E. (1982). A patch-clamp study of bovine chromaffin cells and of their sensitivity to acetylcholine. *Journal of Physiology* **331**, 577–597.

FORSCHER, P. & OXFORD, G. S. (1985). Modulation of calcium channels by norepinephrine in internally dialyzed avian sensory neurons. *Journal of General Physiology* **85**, 743–763.

FRELIN, C., LOMBET, A., VIGNE, P., ROMEY, G. & LAZDUNSKI, M. (1982). Properties of Na channels in fibroblasts. *Biochemical and Biophysical Research Communications* **107**, 202–208.

FUKUSHIMA, Y. & HAGIWARA, S. (1983). Voltage-gated Ca^{2+} channel in mouse myeloma cells. *Proceedings of the National Academy of Sciences of the U.S.A.* **80**, 2240–2242.

FUKUSHIMA, Y., HAGIWARA, S. & SAXTON, R. E. (1984). Variation of calcium current during the cell growth cycle in mouse hybridoma lines secreting immunoglobulins. *Journal of Physiology* **355**, 313–321.

GALLEGO, R. (1983). The ionic basis of action potentials in petrosal ganglion cells of the cat. *Journal of Physiology* **342**, 591–602.

HAGIWARA, S. & BYERLY, L. (1981). Calcium channel. *Annual Review of Neuroscience* **4**, 69–125.

HAGIWARA, S. & KAWA, K. (1984). Calcium and potassium currents in spermatogenic cells dissociated from rat seminiferous tubules. *Journal of Physiology* **356**, 135–149.

HAMILL, O. P., MARTY, A., NEHER, E., SAKMANN, B. & SIGWORTH, F. J. (1981). Improved patch-clamp techniques for high resolution current recording from cells and cell-free membrane patches. *Pflügers Archiv* **391**, 85–100.

HOF, R. P., HOF, A., RUEGG, U. T., COOK, N. S. & VOGEL, A. (1986). Stereoselectivity at the calcium channel: different profiles of hemodynamic activity of the enantiomers of the dihydropyridine derivative PN 200–110. *Journal of Cardiovascular Pharmacology* **8**, 221–226.

JONES, S. J. & BOYDE, A. (1976). Experimental study of changes in osteoblastic shape induced by calcitonin and parathyroid extract in an organ culture system. *Cell Tissue Research* **169**, 449–465.

JONES, S. J. & NESS, A. R. (1977). A study of the arrangement of osteoblasts of rat calvarium cultured in medium with or without added parathyroid extract. *Journal of Cell Science* **25**, 247–263.

LIEBERHERR, M. (1987). Effects of vitamin D_3 metabolites on cytosolic free calcium in confluent mouse osteoblasts. *Journal of Biological Chemistry* **262**, 13168–13173.

LÖWIK, C. W., VAN LEEUWEN, J. P., VAN DER MEER, J. M., VAN ZEELAND, J. K., SCHEVEN, B. A. & HERMANN-ERLEE, M. P. (1985). A two-receptor model for the action of parathyroid hormone on osteoblasts: a role for intracellular free calcium and cAMP. *Cell Calcium* **6**, 311–326.

MCSHEEHY, P. M. & CHAMBERS, T. J. (1986). Osteoblast-like cells in the presence of parathyroid hormone release soluble factor that stimulates osteoblastic bone resorption. *Endocrinology* **119**, 1654–1659.

MACVICAR, B. A. (1984). Voltage-dependent calcium channels in glial cells. *Science* **226**, 1345–1347.

MARCUS, R. & ORNER, F. B. (1980). Parathyroid hormone as a calcium ionophore in bone cells: tests of specificity. *Calcified Tissue International* **32**, 207–211.

MATTESON, D. R. & ARMSTRONG, C. M. (1986). Properties of two types of calcium channels in clonal pituitary cells. *Journal of General Physiology* **87**, 161–182.

MILLER, R. J. (1985). How many types of calcium channels exist in neurones? *Trends in Neurosciences* **8**(2), 45–47.

NARAHASHI, T. (1974). Chemicals as tools in the study of excitable membranes. *Physiological Reviews* **54**, 813–889.

NARAHASHI, T., TSUNOO, A. & YOSHII, M. (1987). Characterization of two types of calcium channels in mouse neuroblastoma cells. *Journal of Physiology* **383**, 231–249.

NEWMAN, E. A. (1985). Voltage-dependent calcium and potassium channels in retinal glial cells. *Nature* **317**, 809–811.

NIJWEIDE, P. J. (1975). Embryonic chicken periosteum in tissue culture: osteid formation and calcium uptake. *Proceedings of the Koninklijke Nederlandse Akademic van Wetenschappen* C**78**, 410.

NILIUS, B., HESS, P., LANSMAN, J. B. & TSIEN, R. W. (1985). A novel type of cardiac calcium channel in ventricular cells. *Nature* **316**, 443–446.

NOWAK, L., ASCHER, P. & BERWALD-NETTER, Y. (1987). Ionic channels in mouse astrocytes in culture. *Journal of Neuroscience* **7**(1), 101–109.

NOWAK, L., ASCHER, P., BERWALD-NETTER, Y. & COURAUD, F. (1983). Single channel currents of cultured mammalian astrocytes studied using excised membrane patches. *Neuroscience Letters* **14**, S264.

NOWYCKY, M. C., FOX, A. P. & TSIEN, R. W. (1985). Three types of neuronal calcium channel with different calcium agonist sensitivity. *Nature* **316**, 440–443.

PERRY, H. M., SKOGEN, W., CHAPPEL, J. C., WILNER, G. D., KAHAN, A. J. & TEITELBAUM, S. L. (1987). Conditioned medium from osteoblast-like cells mediate parathyroid hormone induced bone resorption. *Calcified Tissue International* **40**, 298–300.

PUZAS, J. E. & BRAND, J. S. (1979). Parathyroid hormone stimulation of collagenase secretion by isolated bone cells. *Endocrinology* **104** (2), 559–562.

RODAN, G. A. & MARTIN, T. J. (1981). The role of osteoblasts in hormonal control of bone resorption. *Calcified Tissue International* **33**, 349–351.

RODAN, G. A. & RODAN, S. B. (1984). Expression of the osteoblastic phenotype. In *Bone and Mineral Research*, vol. 2, ed. PECK, W. A., pp. 244–285. Amsterdam: Elsevier Sciences Publishers B.V.

SAKAMOTO, S. & SAKAMOTO, M. (1986). Bone collagenase, osteoblasts and cell-mediated bone resorption. In *Bone and Mineral Research*, vol. 4, ed. PECK, W. A., pp 49–102. Amsterdam: Elsevier Science Publishers B.V.

SCHLICHTER, L., SIDELL, N. & HAGIWARA, S. (1986*a*). K channels are expressed early in human T-cell development. *Proceedings of the National Academy of Sciences of the U.S.A.* **83**, 5625–5629.

SCHLICHTER, L., SIDELL, N. & HAGIWARA, S. (1986*b*). Potassium channels mediate killing by human natural killer cells. *Proceedings of the National Academy of Sciences of the U.S.A.* **83**, 451–455.

SHRAGER, P., CHIU, S. Y. & RITCHIE J. M. (1985). Voltage-dependent sodium and potassium channels in mammalian cultured Schwann cells. *Proceedings of the National Academy of Sciences of the U.S.A.* **82**, 948–952.

SCHRAMM, M., THOMAS, G., TOWART, R. & FRANCKOWIAK, G. (1983). Novel dihydropyridines with positive inotropic action through activation of Ca^{2+} channels. *Nature* **303**, 535–537.

WEISS, R. E. & HORN, R. (1986). Functional differences between two classes of sodium channels in developing rat skeletal muscle. *Science* **233**, 361–364.

WONG, G. L. (1986). Skeletal effects of parathyroid hormone. In *Bone and Mineral Research*, vol. 4, ed. PECK, W. A., pp. 103–129. Amsterdam: Elsevier Science Publishers B.V.

YAARI, Y., HAMON, B. & LUX, H. D. (1987). Development of two types of calcium channels in cultured mammalian hippocampal neurons. *Science* **235**, 680–682.